Applied Mathematical Modelling 45 (2017) 1–13

Contents lists available at ScienceDirect

Applied Mathematical Modelling

journal homepage: www.elsevier.com/locate/apm

Numerical simulation for the solitary wave of Zakharov–Kuznetsov equation based on lattice Boltzmann method

Huimin Wang

College of Applied Mathematics, Jilin University of Finance and Economics, Changchun 130117, PR China

ARTICLE INFO

Article history:
Received 27 November 2014
Revised 27 August 2016
Accepted 14 December 2016
Available online 18 December 2016

Keywords:
Lattice Boltzmann method
Solitary wave
Zakharov–Kuznetsov equation

ABSTRACT

The Zakharov–Kuznetsov equation is considered, which is an equation describing two dimensional weakly nonlinear ion-acoustic waves in plasma. We focus on using the lattice Boltzmann method to study the Zakharov–Kuznetsov equation. A lattice Boltzmann model is constructed. In numerical experiments, the propagation of the single solitary wave and the collision of double solitary waves are simulated. The results with different parameters are investigated and compared.

1. Introduction

In many areas of physics, applied mathematics and engineering, especially in the area of plasma physics, the Zakharov–Kuznetsov (ZK) equation appears [1–3]. The ZK equation was first derived for describing two dimensional weakly nonlinear ion-acoustic waves in strongly magnetized lossless plasma. In a uniform magnetic field, the behavior of weakly nonlinear ion-acoustic waves in a plasma comprised of cold ions and hot isothermal electrons was governed by the ZK equation [3–6]. Many studies have been spent on the traveling wave and soliton solutions of the ZK equation [7–18]. But to obtain an exact solution of such problem is still difficult, so the numerical studies for the ZK equation attract the interest of researchers. In this paper we focus on using the lattice Boltzmann method (LBM) to simulate the weakly nonlinear ion-acoustic solitary waves of the ZK equation.

LBM is a new modeling and simulation method for complex system which has received considerable attention in recent years. It has now become a new tool for computational fluid dynamics. LBM is the inheritance and development of the lattice gas automata (LGA). It is a kind of local dynamic model which is based on the basic theory of nonequilibrium statistical physics and the kinetic theory [19–23]. In this model time, space and particle velocity are all discrete. Different from the traditional numerical methods, LBM needs to solve the mesoscopic kinetic equation of the particle distribution function, then to obtain the macroscopic variables. This makes LBM has many advantages. Nowadays the LBM has been successfully applied in many fields, such as various kinds of flows [24–42], linear and nonlinear partial differential equations [43–58].

In this paper we consider the following ZK equation:

$$\frac{\partial \phi}{\partial t} + \phi \frac{\partial \phi}{\partial \zeta} + \delta \left(\frac{\partial^3 \phi}{\partial \zeta^3} + \frac{\partial^3 \phi}{\partial \eta^2 \partial \zeta} \right) = 0. \tag{1}$$

E-mail addresses: whm780921@sina.com, whm20110605@126.com

http://dx.doi.org/10.1016/j.apm.2016.12.002
0307-904X/

In Section 2, a lattice Boltzmann model for the ZK equation is proposed; in Section 3, the propagation of single solitary wave and the collision of two solitary waves are simulated by using the scheme, numerical results with different parameters are compared; and in Section 4 some conclusions are discussed.

2. Lattice Boltzmann model

2.1. Lattice Boltzmann equation

A two-dimensional lattice is considered to discrete two-dimensional space. "$f_\alpha(\mathbf{x}, t)$" is defined as the single-particle distribution function at time t, position $\mathbf{x}$ with velocity $\mathbf{e}_\alpha$. Suppose that the particle distribution has equilibrium state, "$f_\alpha^{eq}(\mathbf{x}, t)$" is the equilibrium distribution function. The distribution function $f_\alpha(\mathbf{x}, t)$ satisfies the lattice Boltzmann equation

$$f_\alpha(\mathbf{x}+\mathbf{e}_\alpha, t+1) - f_\alpha(\mathbf{x}, t) = -\frac{1}{\tau}\left[f_\alpha(\mathbf{x}, t) - f_\alpha^{eq}(\mathbf{x}, t)\right], \tag{2}$$

where τ is the single relaxation time. Local conservation of 'mass' is assumed, i.e. $f_\alpha^{eq}(\mathbf{x}, t)$ satisfies the conservation condition

$$\sum_\alpha f_\alpha^{eq}(\mathbf{x}, t) = \sum_\alpha f_\alpha(\mathbf{x}, t). \tag{3}$$

Let l represent the mean free path, L represent the characteristic length, and the Knudsen number ε is defined as $\varepsilon = \frac{l}{L}$. Assume that ε is small, replace the time step Δt with ε [43], then the lattice Boltzmann Eq. (2) in physical units can be obtained as follows:

$$f_\alpha(\mathbf{x}+\varepsilon\mathbf{e}_\alpha, t+\varepsilon) - f_\alpha(\mathbf{x}, t) = -\frac{1}{\tau}[f_\alpha(\mathbf{x}, t) - f_\alpha^{eq}(\mathbf{x}, t)]. \tag{4}$$

Furthermore, using the Taylor expansion, multi-scale expansion technique and Chapman–Enskog expansion, a series of partial differential equations in different time scales are obtained [41,42,47,58]. The detailed derivation is given in Appendix A.

2.2. Recovery of the macroscopic equation

The macroscopic quantity is defined by

$$\sum_\alpha f_\alpha(\mathrm{x}, t) = \phi. \tag{5}$$

The moments of the equilibrium distribution function are set as follows:

$$m_1^0 = \frac{1}{2}\phi^2, \tag{6}$$

$$m_2^0 = 0, \tag{7}$$

$$\pi_{11}^0 = \frac{\delta}{\varepsilon C_2}\frac{\partial\phi}{\partial\zeta} + \frac{1}{3}\phi^3, \tag{8}$$

$$\pi_{12}^0 = \pi_{21}^0 = 0, \tag{9}$$

$$\pi_{22}^0 = \frac{\delta}{\varepsilon C_2}\frac{\partial\phi}{\partial\zeta}. \tag{10}$$

Taking (A.5) + $\varepsilon\times$(A.6) and summing it over α, we obtain

$$\frac{\partial\phi}{\partial t} + \phi\frac{\partial\phi}{\partial\zeta} + \delta\left(\frac{\partial^3\phi}{\partial\zeta^3} + \frac{\partial^3\phi}{\partial\eta^2\partial\zeta}\right) = O(\varepsilon^2). \tag{11}$$

Eq. (11) is the recovered approximate calculation formula of Eq. (1). The error analysis is given in the next section.

2.3. The truncation error of the model

Taking (A.5)+$\varepsilon\times$(A.6)+$\varepsilon^2\times$(A.7)+$\varepsilon^3\times$(A.8) and summing it over α, we obtain

$$\frac{\partial\phi}{\partial t}+\phi\frac{\partial\phi}{\partial\zeta}+\delta\left(\frac{\partial^3\phi}{\partial\zeta^3}+\frac{\partial^3\phi}{\partial\eta^2\partial\zeta}\right)=E_2+E_3+O(\varepsilon^4). \tag{12}$$

In Eq. (12), E_2 and E_3 are the second and third-order error terms respectively.
In this model, we use the two-dimensional 5-bit lattice

$$e_\alpha=\begin{cases}c\left[\cos\frac{(\alpha-1)\pi}{2},\sin\frac{(\alpha-1)\pi}{2}\right], & \alpha=1,\ldots,4,\\ 0, & \alpha=0.\end{cases} \tag{13}$$

For two-dimensional 5-bit lattice (13), we have

$$P^0_{111}=c^2m^0_1, \tag{14}$$

$$P^0_{222}=c^2m^0_2, \tag{15}$$

$$Q^0_{1111}=c^2\pi^0_{11}, \tag{16}$$

$$Q^0_{2222}=c^2\pi^0_{22}, \tag{17}$$

$$\begin{aligned}E_2&=-\varepsilon^2\left(C_3\sum_\alpha\Delta^3f^{(0)}_\alpha+2C_2\sum_\alpha\Delta\frac{\partial}{\partial t_1}f^{(0)}_\alpha\right)\\&=-\varepsilon^2C_3\sum_\alpha\Delta^3f^{(0)}_\alpha\\&=-\varepsilon^2C_3\left(\frac{\partial^3\phi}{\partial t_0^3}+3\frac{\partial^3m^0_j}{\partial t_0^2\partial x_j}+3\frac{\partial^3\pi^0_{ij}}{\partial t_0\partial x_i\partial x_j}+\frac{\partial^3P^0_{ijk}}{\partial x_i\partial x_j\partial x_k}\right)\\&=-\varepsilon^2C_3\left[-\frac{\delta}{2\varepsilon C_2}\frac{\partial^4\phi^2}{\partial\zeta^4}-\frac{\delta}{2\varepsilon C_2}\frac{\partial^4\phi^2}{\partial\zeta^2\partial\eta^2}+\frac{\partial^3}{\partial\zeta^3}\left(\frac{c^2}{2}\phi^2-\frac{1}{4}\phi^4\right)\right],\end{aligned} \tag{18}$$

$$\begin{aligned}E_3&=-\varepsilon^3\left(C_4\sum_\alpha\Delta^4f^{(0)}_\alpha+3C_3\sum_\alpha\Delta^2\frac{\partial}{\partial t_1}f^{(0)}_\alpha+2C_2\sum_\alpha\Delta\frac{\partial}{\partial t_2}f^{(0)}_\alpha+C_2\frac{\partial^2}{\partial t_1^2}\sum_\alpha f^{(0)}_\alpha\right)\\&=-\varepsilon^3\left[\frac{\partial^4}{\partial\zeta^4}\left(\frac{3C_4}{5}\phi^5-C_4c^2\phi^3\right)+\frac{C_4\delta}{\varepsilon C_2}\left(\frac{\partial^5\phi^3}{\partial\zeta^5}+\frac{\partial^5\phi^3}{\partial\zeta^3\partial\eta^2}\right)+\frac{C_4c^2\delta}{\varepsilon C_2}\left(\frac{\partial^5\phi}{\partial\zeta^5}+\frac{\partial^5\phi}{\partial\zeta\partial\eta^4}\right)\right.\\&\quad\left.-\frac{\delta^2(3C_3-C_2^2)}{\varepsilon^2C_2}\left(\frac{\partial^6\phi}{\partial\zeta^6}+2\frac{\partial^6\phi}{\partial\zeta^4\partial\eta^2}+\frac{\partial^6\phi}{\partial\zeta^2\partial\eta^4}\right)\right].\end{aligned} \tag{19}$$

Thus, the macroscopic equation can be recovered as:

$$\frac{\partial\phi}{\partial t}+\phi\frac{\partial\phi}{\partial\zeta}+\delta\left(\frac{\partial^3\phi}{\partial\zeta^3}+\frac{\partial^3\phi}{\partial\eta^2\partial\zeta}\right)=O(\varepsilon). \tag{20}$$

For the two-dimensional 5-bit lattice (13), based on Eqs. (5)–(10), we obtain the expression of the equilibrium distribution function

$$f^{(0)}_\alpha=\begin{cases}\frac{\phi^2}{4c}+\frac{\delta}{2\varepsilon C_2c^2}\frac{\partial\phi}{\partial\zeta}+\frac{1}{6c^2}\phi^3, & \alpha=1,\\ \frac{\delta}{2\varepsilon C_2c^2}\frac{\partial\phi}{\partial\zeta}+\frac{1}{6c^2}\phi^3-\frac{\phi^2}{4c}, & \alpha=2,\\ \frac{\delta}{2\varepsilon C_2c^2}\frac{\partial\phi}{\partial\zeta}, & \alpha=3,\\ \frac{\delta}{2\varepsilon C_2c^2}\frac{\partial\phi}{\partial\zeta}, & \alpha=4,\\ \phi-\frac{2\delta}{\varepsilon C_2c^2}\frac{\partial\phi}{\partial\zeta}-\frac{1}{3c^2}\phi^3, & \alpha=0.\end{cases} \tag{21}$$

3. Numerical example

In this section, some numerical examples are given to examine the efficiency of the lattice Boltzmann model. We use the scheme to simulate the propagation of the single solitary wave and the collision of double solitary waves in the ZK equation.

Example 1. *Propagation of the single solitary wave*

Assume that the initial condition has the following form [18]:

$$\phi(\zeta,\eta,0)=3a\ sech^2\left[0.5\sqrt{\frac{a}{\delta}}(\zeta\cos\theta+\eta\sin\theta)\right]. \tag{22}$$

The boundary conditions are given by

$$\phi(\zeta_A,\eta,t)=3a\ sech^2\left\{0.5\sqrt{\frac{a}{\delta}}[(\zeta_A-at)\cos\theta+\eta\sin\theta]\right\}, \tag{23}$$

$$\phi(\zeta,\eta_A,t)=3a\ sech^2\left\{0.5\sqrt{\frac{a}{\delta}}[(\zeta-at)\cos\theta+\eta_A\sin\theta]\right\}, \tag{24}$$

where ζ_A, η_A represent the boundary points. The computing domain is $(\zeta,\eta)\in[-5,5]^2$, $\delta=0.01$, $a=0.1$, $\theta=0$. The propagation of the solitary wave solution and contour plot for the electric field potential ϕ with initial condition (22) are shown in Fig. 1(a)–(f) and Fig. 2(a)–(f). The parameters are lattice size $M\times N=100\times100$, $\Delta t=0.001$, $\Delta\zeta=\Delta\eta=10/M$, $c=\Delta\zeta/\Delta t$, $\tau=1.09$. In Fig. 3, we plot the curve of the error $Er=|\phi^N-\phi^E|$ at $\eta=0$, where φ^N is the numerical solution, φ^E is the exact solution and φ^E [18] is

$$\phi(\zeta,\eta,t)=3a\ sech^2\left\{0.5\sqrt{\frac{a}{\delta}}[(\zeta-at)\cos\theta+\eta\sin\theta]\right\}. \tag{25}$$

The results show that the numerical solution is consistent with the exact solution and the result is agreeable. We also plot the curve of the infinite norm of the error $||Er||_\infty$ versus the Knudsen number ε, see Figs. 4 and 5, here $||Er||_\infty=\max_{(i,j)}\{Er\}$. Fig. 4 is for the fixed c, $c=100.0$; Fig. 5 is for the fixed lattice size, $M=N=100.0$, $t=5.0$. By using the regression fitting, we obtain the fitting curve. The slope of the curve represents the convergence order of the model. Fig. 4(a) shows the fitting curve at $t=2$, the slope is 1.40784; Fig. 4(b) shows the fitting curve at $t=5$, the slope is 1.60825. In our model, the Knudsen ε equals to the time step Δt and the space step $\Delta\zeta=\Delta\eta=c\Delta t=c\varepsilon$. So for the fixed parameter c, the slope represents the convergence order of the model in time and in space. The figures show the model is convergent. Figs. 4 and 5 also show the dependence relation between the truncation error and the number ε. To get more information, a number of numerical experiments are conducted. In Tables 1 and 2, the comparisons of infinite norm of the error $\|Er\|_\infty$ with different lattice sizes for the fixed c are listed. Table 1 is for $t=2$, $c=100.0$; Table 2 is for $t=5$, $c=100.0$. We found that there exists some critical number, when the lattice size M is less than the critical number, the infinite norm of the error reduces as the lattice size increases; when the lattice size M is more than the critical number, the infinite norm of the error no longer decreases with the increase of the lattice size but increases. For different times t, the critical number is different. We also study the relation between the error and the time step keeping the lattice size same. Table 3 lists the comparison of infinite norm of the error with different time steps for the fixed lattice size, $M=N=100$, $t=5$. The infinite norm of the error decreases with the decrease of the time step, once the time step is less than some critical number, the infinite norm of the error no longer decreases but increases gradually.

To test the effectivity of the lattice Boltzmann model, we also simulate the solitary waves by using the explicit difference scheme and the 4th-order Runge–Kutta scheme. The numerical results by different schemes are compared. The explicit scheme we use is

$$\begin{aligned}\phi_{i,j}^{n+1}=\phi_{i,j}^{n}-\Bigg[&\phi_{i,j}^{n}\frac{\phi_{i+1,j}^{n}-\phi_{i-1,j}^{n}}{2\Delta\zeta}+\delta\frac{\phi_{i+2,j}^{n}-2\phi_{i+1,j}^{n}+2\phi_{i-1,j}^{n}-\phi_{i-2,j}^{n}}{2(\Delta\zeta)^3}\\&+\delta\frac{\phi_{i+1,j+1}^{n}-2\phi_{i+1,j}^{n}+\phi_{i+1,j-1}^{n}-\phi_{i-1,j+1}^{n}+2\phi_{i-1,j}^{n}-\phi_{i-1,j-1}^{n}}{2\Delta\zeta(\Delta\eta)^2}\Bigg]\Delta t.\end{aligned} \tag{26}$$

In the 4th-order Runge–Kutta scheme we considered, Eq. (1) is rewritten as the following form:

$$\frac{\partial\phi}{\partial t}=-\phi\frac{\partial\phi}{\partial\zeta}-\delta\left(\frac{\partial^3\phi}{\partial\zeta^3}+\frac{\partial^3\phi}{\partial\eta^2\partial\zeta}\right)=f(t_n,\phi_{i,j}^{n}). \tag{27}$$

The quantity $\phi_{i,j}^{n+1}$ at $(n+1)$th time step and the space grid (i,j) is obtained by that at nth time step

$$\phi_{i,j}^{n+1}=\phi_{i,j}^{n}+\frac{\Delta t}{6}(k_1+k_2+k_3+k_4), \tag{28}$$

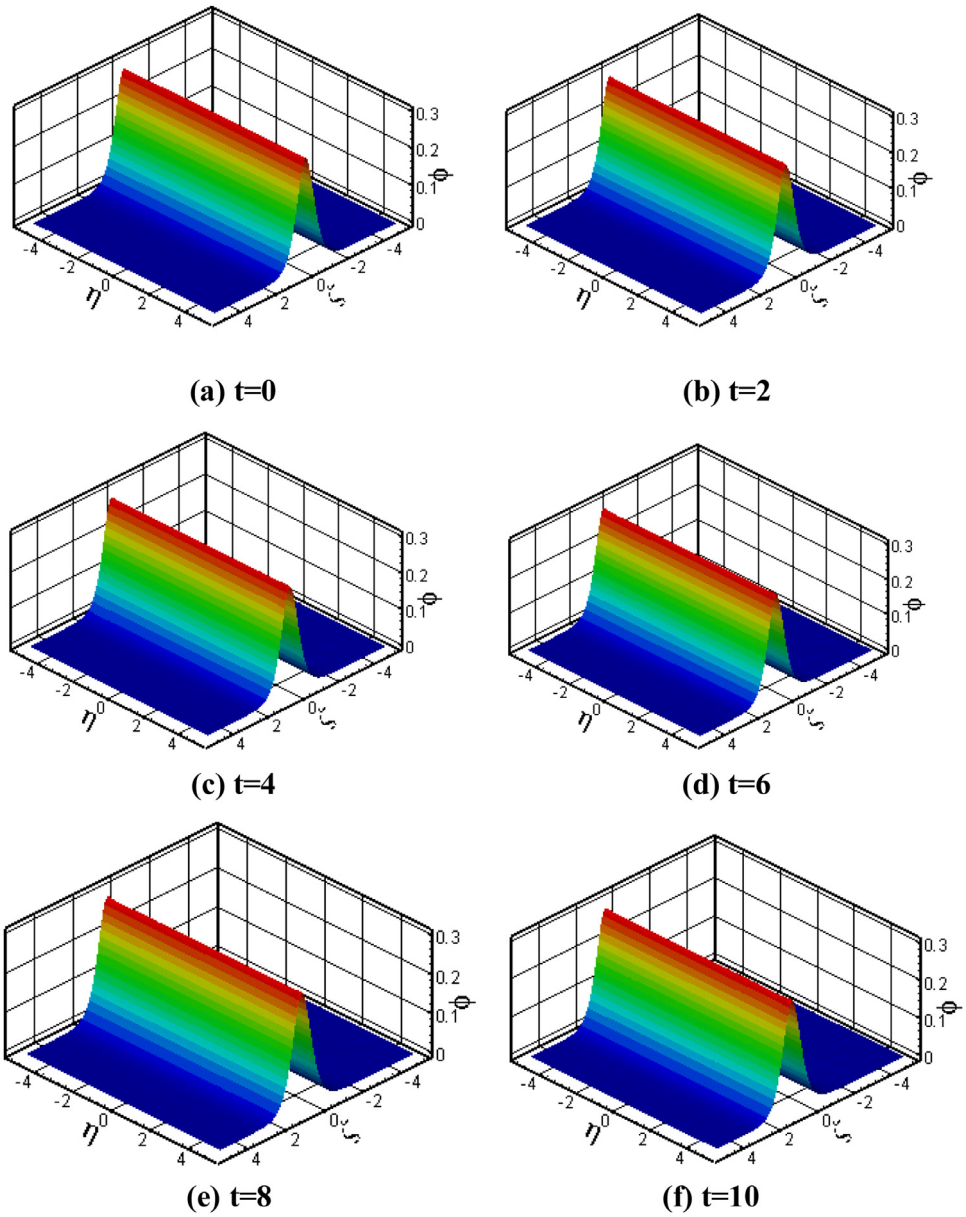

Fig. 1. The propagation of the bright solitary wave for electric field potential ϕ with initial condition (22).

$$f(t_n,\phi_{i,j}^n) = -\left[\phi_{i,j}^n \frac{\phi_{i+1,j}^n - \phi_{i-1,j}^n}{2\Delta\zeta} + \delta \frac{\phi_{i+2,j}^n - 2\phi_{i+1,j}^n + 2\phi_{i-1,j}^n - \phi_{i-2,j}^n}{2(\Delta\zeta)^3} + \delta \frac{\phi_{i+1,j+1}^n - 2\phi_{i+1,j}^n + \phi_{i+1,j-1}^n - \phi_{i-1,j+1}^n + 2\phi_{i-1,j}^n - \phi_{i-1,j-1}^n}{2\Delta\zeta(\Delta\eta)^2}\right], \tag{29}$$

$$k_1 = f(t_n,\phi_{i,j}^n), \tag{30}$$

$$k_2 = f\left(t_n + \frac{\Delta t}{2}, \phi_{i,j}^n + \frac{\Delta t}{2}k_1\right), \tag{31}$$

$$k_3 = f\left(t_n + \frac{\Delta t}{2}, \phi_{i,j}^n + \frac{\Delta t}{2}k_2\right), \tag{32}$$

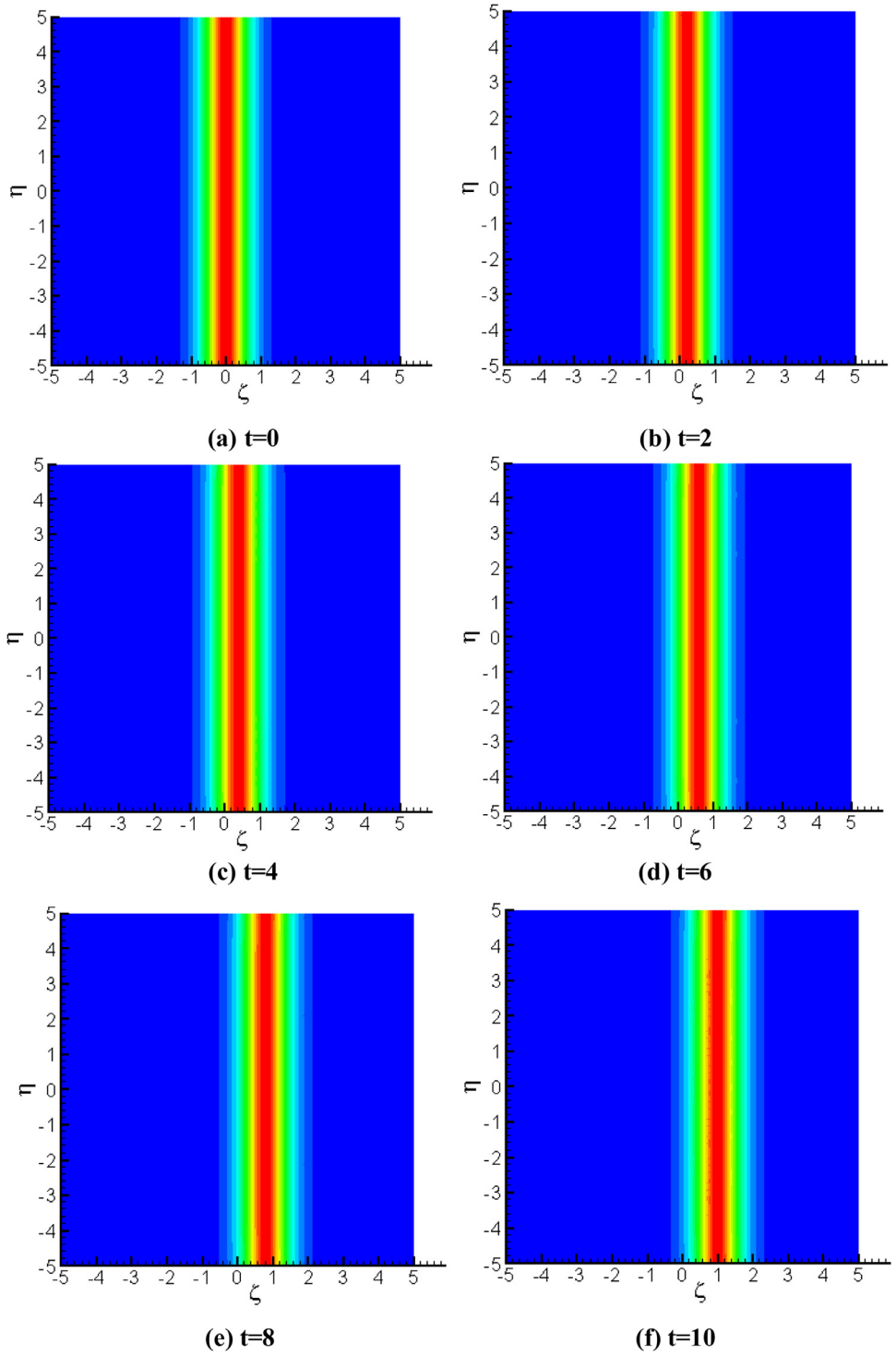

Fig. 2. The contour plot for electric field potential ϕ with initial condition (22).

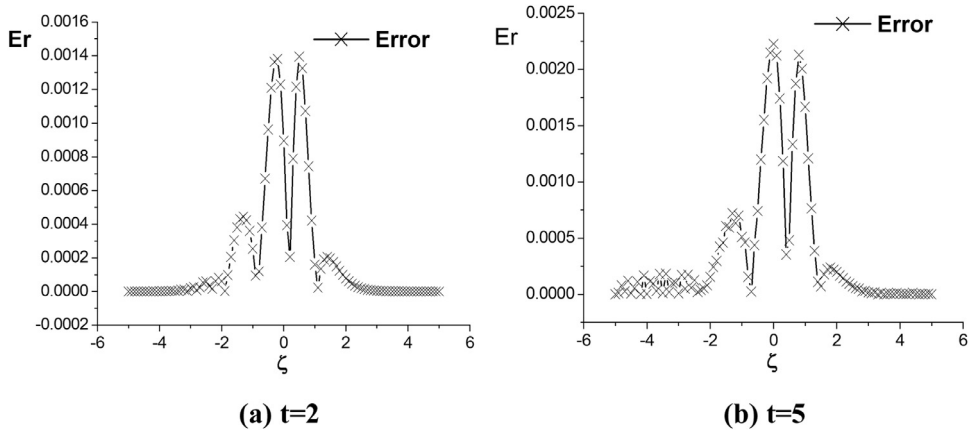

Fig. 3. The curve of LBM model error at $\eta = 0$.

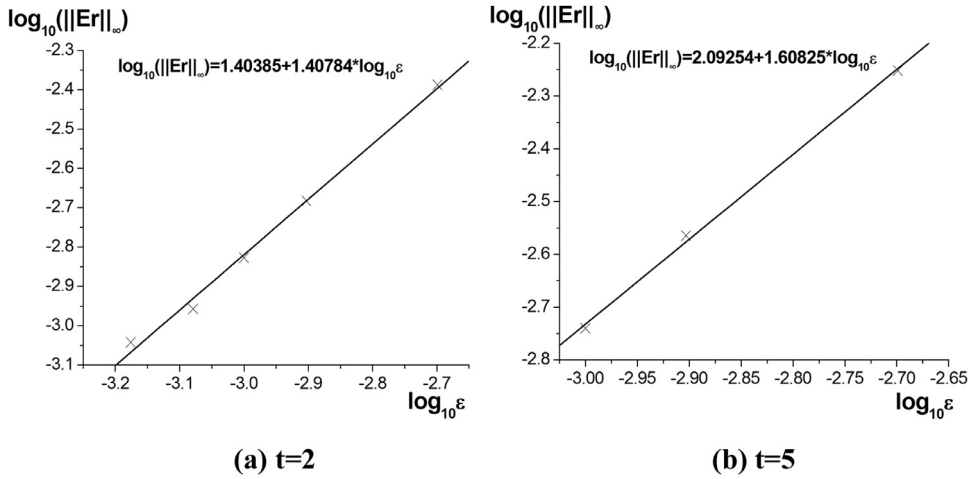

Fig. 4. The curve of the infinite norm of the error $\|Er\|_\infty$ versus the Knudsen number ε for the fixed c. (a) The slope is 1.40784, $t=2$; (b) the slope is 1.60825, $t=5$.

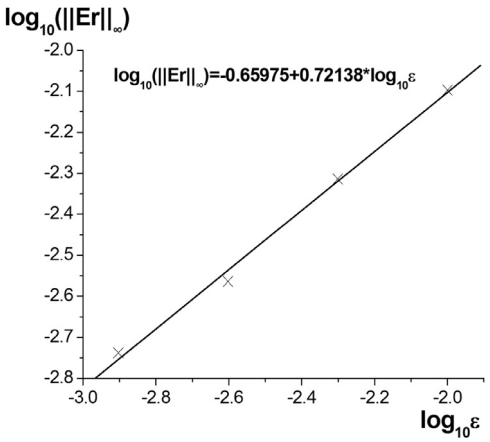

Fig. 5. The curve of the infinite norm of the error $\|Er\|_\infty$ versus the Knudsen number ε for the fixed lattice size, $M \times N = 100 \times 100$, $t=5$. The slope is 0.72138.

Table 1
The comparison of infinite norm of the error with different lattice sizes at $t=2$ for the fixed c, $c=100.0$.

$M\times N$	50×50	80×80	100×100	120×120
$\|\|E_r\|\|_\infty$	4.094437E–03	2.074614E–03	1.488417E–03	1.102984E–03
$M\times N$	150×150	160×160	200×200	
$\|\|E_r\|\|_\infty$	9.080616E–04	9.546429E–04	1.541629E–03	

Table 2
The comparison of infinite norm of the error with different lattice sizes at $t=5$ for the fixed c, $c=100.0$.

$M\times N$	50×50	80×80	100×100	120×120
$\|\|E_r\|\|_\infty$	5.599171E–03	2.725601E–03	1.818806E–03	2.172723E–03
$M\times N$	150×150	200×200	400×400	
$\|\|E_r\|\|_\infty$	3.512219E–03	5.134867E–03	1.270771E–02	

Table 3
The comparison of infinite norm of the error with different time steps for the fixed lattice size, $M\times N=100\times 100$, $t=5$.

Δt	0.01	0.005	0.0025	0.00125
$\|\|E_r\|\|_\infty$	7.996053E–03	4.850954E–03	2.729014E–03	1.829326E–03
Δt	0.000625	0.005	0.00025	0.000125
$\|\|E_r\|\|_\infty$	1.840651E–03	1.841813E–03	1.842588E–03	1.849756E–03

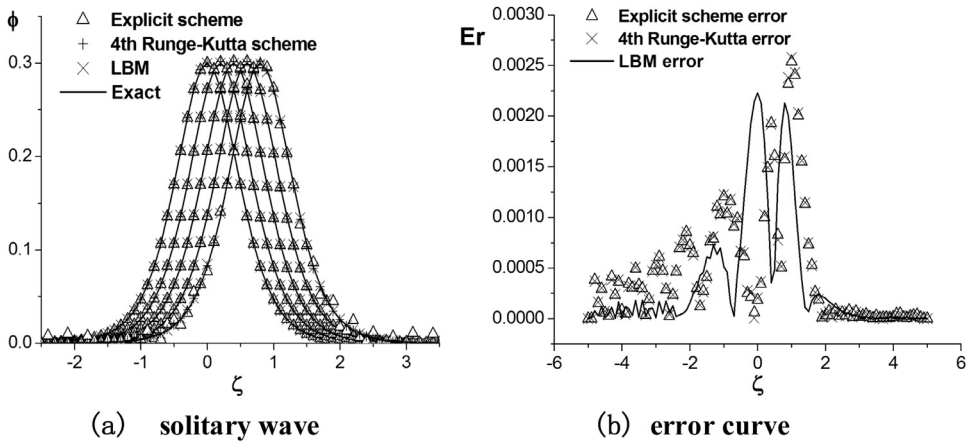

Fig. 6. The comparison of numerical results by different numerical schemes at $\eta=0$.

$$k_4 = f\left(t_n + \Delta t, \phi_{i,j}^n + \Delta t\ k_3\right). \tag{33}$$

In Fig. 6, we plot the comparison curves of the numerical solutions by three schemes. Fig. 6(a) is the solitary waves at $\eta=0$ for $t=0$, $t=2$, $t=4$, $t=6$, $t=8$ and (b) is the error curves at $\eta=0$ for $t=5$. In Tables 4–6, we give the comparison of $\|Er\|_\infty$ at different times with different lattice sizes of numerical solutions by three schemes. It is shown that the simulation result by the lattice Boltzmann model is better than that by the explicit scheme, similar and slightly better than the 4th-order Runge–Kutta scheme. The results show that the solitary wave by the lattice Boltzmann model with these several lattice sizes all can be conserved for a long time. When the lattice size is set as some smaller numbers, such as $M=N=50$, 80, 100, the solitary waves by the explicit scheme and the 4th-order Runge–Kutta scheme are conserved in a longer period of time. But for $M=150$ and$M=200$, the solitary waves by the explicit scheme and the 4th-order Runge–Kutta scheme only can be conserved in a shorter period of time. For$M=150$, the solitary wave by the explicit scheme can't be conserved to $t=1$, the solitary wave by the 4th-order Runge–Kutta scheme cannot be conserved to $t=5$. For $M=200$, the solitary wave by the explicit scheme cannot be conserved to $t=0.2$, the solitary wave by the 4th-order Runge–Kutta scheme cannot be conserved to $t=1$. In the sensitivity of conserving solitary wave to M, the explicit scheme and the 4th-order Runge–Kutta scheme are more dependent on the lattice size than the lattice Boltzmann model. In Table 7, the comparison of the CPU time of different schemes is listed. The explicit scheme takes a minimum CPU time but the accuracy is the lowest. The

Table 4
The comparison of infinite norm of the error at different times of different schemes, $\Delta t = 0.001$.

M	Model	$t=2$	$t=4$	$t=6$	$t=8$	$t=10$
50	Explicit	6.644398E–03	8.955687E–03	1.245688E–02	1.598206E–02	1.961981E–02
	Runge–Kutta	6.631196E–03	8.977711E–03	1.249345E–02	1.602289E–02	1.966260E–02
	LBM	4.096687E–03	5.319893E–03	6.075382E–03	6.770685E–03	7.450849E–03
80	Explicit	2.381690E–03	3.585979E–03	4.795194E–03	6.333873E–03	7.590666E–03
	Runge–Kutta	2.397161E–03	3.618956E–03	4.828826E–03	6.373376E–03	7.639393E–03
	LBM	2.082586E–03	2.563611E–03	2.769530E–03	3.152490E–03	3.225565E–03
100	Explicit	1.507323E–03	2.304807E–03	3.190756E–03	1.525642E–02	6.582087E–01
	Runge–Kutta	1.522679E–03	2.331913E–03	3.110468E–03	4.068509E–03	4.782706E–03
	LBM	1.488715E–03	1.752764E–03	1.951575E–03	2.784416E–03	4.236877E–03
150	LBM	1.040980E–03	3.143862E–03	5.581126E–03	8.281946E–03	1.100832E–02
200	LBM	2.347603E–03	5.723402E–03	9.483412E–03	1.272997E–02	1.770057E–02

Table 5
The comparison of infinite norm of the error at different times by the explicit scheme, $\Delta t = 0.001$.

M	$t=0.1$	$t=0.2$	$t=0.8$	$t=0.9$	$t=1$
150	8.836389E–05	1.671314E–04	1.546635E–02	1.094656E–01	7.867501E–01
200	7.984042E–05	1.006121			

Table 6
The comparison of infinite norm of the error $\|Er\|_\infty$ at different times by the 4th-order Runge–Kutta scheme, $\Delta t = 0.001$.

M	$t=1$	$t=2$	$t=3$	$t=4$	$t=5$
150	5.758554E–04	6.721169E–04	9.870678E–04	9.361282E–03	1.985978E–01
200	2.830675E–01				

Table 7
The comparison of CPU time (s) of different schemes, $\Delta t = 0.001$.

M	Model	$t=2$	$t=4$	$t=6$	$t=8$	$t=10$
50	Explicit	2	5	6	9	11
	Runge–Kutta	7	12	18	24	32
	LBM	5	9	14	18	23
80	Explicit	5	10	14	19	23
	Runge–Kutta	14	28	42	55	69
	LBM	11	22	31	45	51
100	Explicit	8	14	21	28	35
	Runge–Kutta	23	47	69	92	119
	LBM	16	31	47	63	78

accuracy of the lattice Boltzmann model is slightly higher than that of the 4th-order Runge–Kutta scheme and takes much less CPU time.

Example 2. *Collision of double solitary waves*

Assume that the initial condition has the following form [18]:

$$\phi(\zeta,\eta,0)=\sum_{j=1}^{2}3a_j sech^2\left\{0.5\sqrt{\frac{a_j}{\delta}}[(\zeta-\zeta_j)\cos\theta+(\eta-\eta_j)\sin\theta]\right\}. \tag{34}$$

The boundary conditions are given by

$$\phi(\zeta_A,\eta,t)=\phi(\zeta_A+\Delta\zeta,\eta,t), \tag{35}$$

$$\phi(\zeta,\eta_A,t)=\phi(\zeta,\eta_A+\Delta\eta,t), \tag{36}$$

where ζ_A, η_A represent the boundary points. The computing domain is $(\zeta,\ \eta)\in[0,\ 8]^2$, and the parameters are $a_1=0.45$, $a_2=0.25$, $\delta=0.01$, $\zeta_1=2.5$, $\eta_1=0$, $\zeta_2=3.3$, $\eta_2=0$, $\theta=0$, lattice size $M\times N=100\times100$, $\Delta t=0.001$, $\Delta\zeta=\Delta\eta=8/M$, $c=\Delta\zeta/\Delta t$, $\tau=1.1$. The collision of double solitary waves and contour plot for the electric field potential ϕ with initial condition (34) are shown in Fig. 7(a)–(d) and Fig. 8(a)–(d).

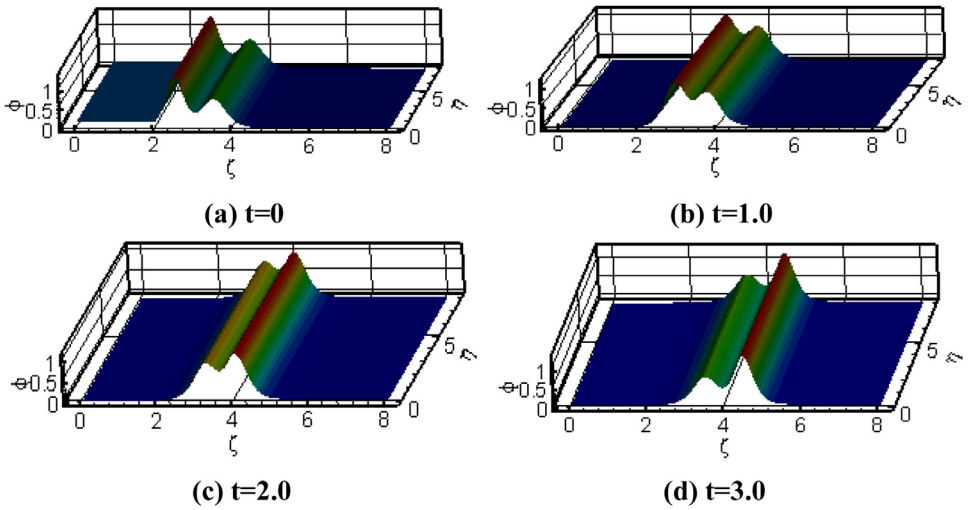

Fig. 7. The collision of double solitary waves for electric field potential ϕ with initial condition (34).

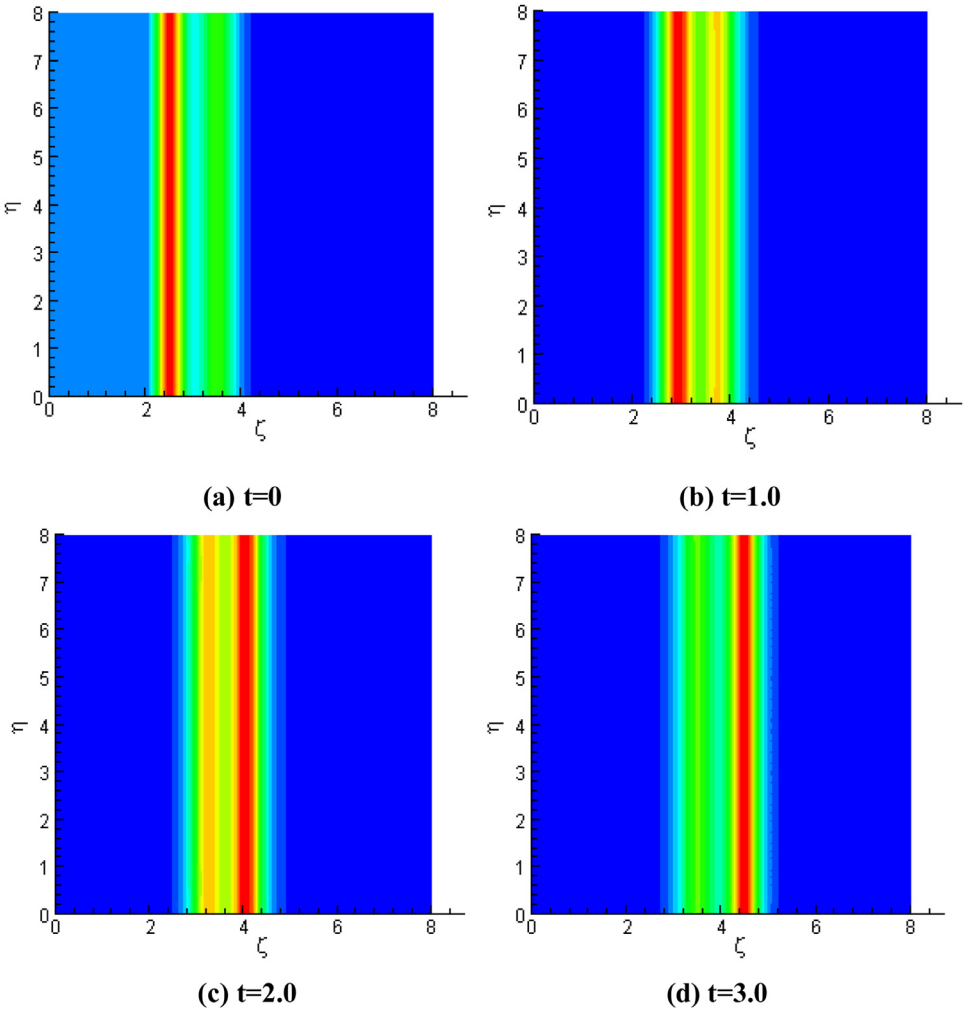

Fig. 8. The contour plot for electric field potential ϕ with initial condition (34).

4. Conclusion

In this paper, we propose a lattice Boltzmann model for the ZK equation by using a series of lattice Boltzmann equations in the different time scales. We simulate the propagation of single solitary wave and the collision of double solitary waves. The results show that LBM is an effective method to simulate the solitary waves of ZK equation. In our future works we should further consider the three dimensional ZK equation.

Acknowledgments

This work is supported by the "13th Five-Year" Science and Technology Research Project of the Education Department of Jilin Province (No. 2016101); the Youth Project of Jilin University of Finance and Economics (No. XJ2012003).

Appendix A

Using the Taylor expansion on Eq. (4), and retaining terms up to $O(\varepsilon^4)$, we have

$$f_\alpha(\mathbf{x}+\varepsilon e_\alpha, t+\varepsilon) - f_\alpha(\mathbf{x},t) = \sum_{n=1}^{4} \frac{\varepsilon^n}{n!}\left(\frac{\partial}{\partial t} + \mathbf{e}_\alpha \frac{\partial}{\partial \mathbf{x}}\right)^n f_\alpha(\mathbf{x},t) + O(\varepsilon^5). \tag{A.1}$$

The Chapman–Enskog expansion can be applied to f_α under the assumption of the small Knudsen number [59]

$$f_\alpha^\sigma = f_\alpha^{(0)} + \sum_{n=1}^{\infty} \varepsilon^n f_\alpha^{(n)}, \tag{A.2}$$

where $f_\alpha^{(0)} \equiv f_\alpha^{eq}$. Introducing t_0, t_1, t_2, t_3 as different scale times, we define them as:

$$t_i = \varepsilon^i t, i = 0, 1, 2, 3, \tag{A.3}$$

and

$$\frac{\partial}{\partial t} = \sum_{n=0}^{3} \varepsilon^n \frac{\partial}{\partial t_n} + O(\varepsilon^4). \tag{A.4}$$

Combining the Eqs. (A.1)–(A.4), equations to other orders in ε are as follows:

$$C_1 \Delta f_\alpha^{(0)} = -\frac{1}{\tau} f_\alpha^{(1)}, \tag{A.5}$$

$$\frac{\partial}{\partial t_1} f_\alpha^{(0)} + C_2 \Delta^2 f_\alpha^{(0)} = -\frac{1}{\tau} f_\alpha^{(2)}, \tag{A.6}$$

$$C_3 \Delta^3 f_\alpha^{(0)} + 2C_2 \Delta \frac{\partial}{\partial t_1} f_\alpha^{(0)} + \frac{\partial}{\partial t_2} f_\alpha^{(0)} = -\frac{1}{\tau} f_\alpha^{(3)}, \tag{A.7}$$

$$C_4 \Delta^4 f_\alpha^{(0)} + 3C_3 \Delta^2 \frac{\partial}{\partial t_1} f_\alpha^{(0)} + 2C_2 \Delta \frac{\partial}{\partial t_2} f_\alpha^{(0)} + \frac{\partial}{\partial t_3} f_\alpha^{(0)} + C_2 \frac{\partial^2}{\partial t_1^2} f_\alpha^{(0)} = -\frac{1}{\tau} f_\alpha^{(4)}, \tag{A.8}$$

where the partial differential operator $\Delta \equiv \frac{\partial}{\partial t_0} + e_\alpha \frac{\partial}{\partial \mathbf{x}}$.

Eqs. (A.5)–(A.8) are so-called series of partial differential equations in different time scales [48]. In Eqs. (A.5)–(A.8), C_i are polynomials of the single relaxation time τ.

$$C_1 = 1, \tag{A.9}$$

$$C_2 = \frac{1}{2} - \tau, \tag{A.10}$$

$$C_3 = \tau^2 - \tau + \frac{1}{6}, \tag{A.11}$$

$$C_4 = -\tau^3 + \frac{3}{2}\tau^2 - \frac{7}{12}\tau + \frac{1}{24}. \tag{A.12}$$

Combining the conservation condition (3) and Eq. (A.2), which yields

$$\sum_\alpha f_\alpha^{(n)}(\mathbf{x},t) = 0, \text{ for } n \geq 1. \tag{A.13}$$

Eq. (A.13) means that moment 0 vanishes in each order $n \geq 1$ of ε.
Some moments of the equilibrium distribution functions are denoted as follows:

$$\sum_{\alpha} f_{\alpha}^{(0)}(\mathrm{x}, t) e_{\alpha j} \equiv m_j^0(\mathbf{x}, t), \tag{A.14}$$

$$\sum_{\alpha} f_{\alpha}^{(0)}(\mathrm{x}, t) e_{\alpha i} e_{\alpha j} \equiv \pi_{ij}^0(\mathbf{x}, t), \tag{A.15}$$

$$\sum_{\alpha} f_{\alpha}^{(0)}(\mathrm{x}, t) e_{\alpha i} e_{\alpha j} e_{\alpha k} \equiv P_{ijk}^0(\mathbf{x}, t), \tag{A.16}$$

$$\sum_{\alpha} f_{\alpha}^{(0)}(\mathrm{x}, t) e_{\alpha i} e_{\alpha j} e_{\alpha k} e_{\alpha l} \equiv Q_{ijkl}^0(\mathbf{x}, t). \tag{A.17}$$

Summing Eq. (A.5) over α, we obtain:

$$\frac{\partial \phi}{\partial t_0} + \frac{\partial m_j^0}{\partial x_j} = 0. \tag{A.18}$$

Eq. (A.18) is so-called conservation law in time scale t_0.

References

[1] J. Das, A. Bandyopadhyay, K.P. Das, Existence and stability of alternatives ion-acoustic solitary wave solution of the combined MKdV–KdV–ZK equation in a magnetized nonthermal plasma consisting of warm adiabatic ions, Phys. Plasmas 14 (9) (2007) 092304.
[2] C. Lin, X. Zhang, The formally variable separation approach for the modified Zakharov–Kuznetsov equation, Commun. Nonlinear Sci. Numer. Simul. 12 (5) (2007) 636–642.
[3] A. Mushtaq, H.A. Shah, Nonlinear Zakharov–Kuznetsov equation for obliquely propagating two-dimensional ion-acoustic solitary waves in a relativistic, rotating magnetized electron–positron–ion plasma, Phys. Plasmas 12 (7) (2005) 072306.
[4] X. Lü, B. Tian, T. Xu, K.J. Cai, W.J. Liu, Analytical study of the nonlinear Schrödinger equation with an arbitrary linear time-dependent potential in quasi-one-dimensional Bose–Einstein condensates, Ann. Phys. 323 (10) (2008) 2554–2565.
[5] X. Lü, H.W. Zhu, Z.Z. Yao, X.H. Meng, C. Zhang, C.Y. Zhang, B. Tian, Multisoliton solutions in terms of double Wronskian determinant for a generalized variable-coefficient nonlinear Schrödinger equation from plasma physics, arterial mechanics, fluid dynamics and optical communications, Ann. Phys. 323 (8) (2008) 1947–1955.
[6] A. Biswas, E. Zerrad, Solitary wave solution of the Zakharov–Kuznetsov equation in plasmas with power law nonlinearity, Nonlinear Anal-Real 11 (2010) 3272–3274.
[7] I. Kourakis, W.M. Moslem, U.M. Abdelsalam, R. Sabry, P.K. Shukla, Nonlinear dynamics of rotating multi-component pair plasmas and e-p-i plasmas, Plasma Fusion Res. 4 (2009) 1–11.
[8] E. Infeld, P. Fryczs, Self-focusing of nonlinear ion-acoustic waves and solitons in magnetized plasmas. Part 2. Numerical simulations, two-soliton collisions, J. Plasma Phys. 37 (1987) 97–106.
[9] J.H. He, Application of homotopy perturbation method to nonlinear wave equations, Chaos Solitons Fractals 26 (2005) 695–700.
[10] Q. Qu, B. Tian, W. Liu, K. Sun, P. Wang, Y. Jiang, B. Qin, Soliton solutions and interactions of the Zakharov–Kuznetsov equation in the electron—positron–ion plasmas, Eur. Phys. J. D. 61 (2011) 709–715.
[11] B. Zhang, Z. Liu, Q. Xiao, New exact solitary wave and multiple soliton solutions of quantum Zakharov–Kuznetsov equation, Appl. Math. Comput. 217 (2010) 392–402.
[12] F. Awawdeh, New exact solitary wave solutions of the Zakharov–Kuznetsov equation in the electron–positron–ion plasmas, Appl. Math. Comput. 218 (2012) 7139–7143.
[13] A.R. Seadawy, New exact solutions for the KdV equation with higher order nonlinearity by using the variational method, Comput. Appl. Math. 62 (2011) 3741–3755.
[14] A.R. Seadawy, Traveling wave solutions of the Boussinesq and generalized fifth-order KdV equations by using the direct algebraic method, Appl. Math. Sci. 6 (2012) 4081–4090.
[15] A.R. Seadawy, K.E.I. Rashidy, Traveling wave solutions for some coupled nonlinear evolution equations, Math. Comput. Model. 57 (2013) 1371–1379.
[16] D. Kumar, J. Singh, S. Kumar, Numerical computation of nonlinear fractional Zakharov–Kuznetsov equation arising in ion-acoustic waves, J. Egypt. Math. Soc. 22 (3) (2013) 1–6.
[17] A.R. Seadawy, Stability analysis for Zakharov–Kuznetsov equation of weakly nonlinear ion-acoustic waves in a plasma, Comput. Math. Appl. 67 (2014) 172–180.
[18] X. Qian, S.H. Song, E. Gao, W.B. Li, Explicit multi-symplectic method for the Zakharov–Kuznetsov equation, Chin. Phys. B 21 (2012) 070206.
[19] S.Y. Chen, G.D. Doolen, Lattice Boltzmann method for fluid flows, Ann. Rev. Fluid Mech. 30 (1998) 329–364.
[20] Y.H. Qian, D. d'Humieres, P. Lallemand, Lattice BGK Models for Navier–Stokes Equations, Europhys. Lett. 17 (6) (1992) 479–484.
[21] F. Higuera, S. Succi, R. Benzi, Lattice gas dynamics with enhanced collisions, Europhys. Lett. 9 (1989) 345–349.
[22] R. Benzi, S. Succi, M. Vergassola, The lattice Boltzmann equation: theory and Applications, Phys. Rep. 222 (1992) 147–197.
[23] S. Succi, R. Benzi, Lattice Boltzmann equation for quantum mechanics, Physica D 69 (1993) 327–332.
[24] M. Mendoza, B.M. Boghosian, H.J. Herrmann, S. Succi, Fast lattice Boltzmann solver for relativistic hydrodynamics, Phys. Rev. Lett. 105 (2010) 014502.
[25] L.S. Luo, Theory of the lattice Boltzmann method: lattice Boltzmann method for nonideal gases, Phys. Rev. E 62 (2000) 4982–4996.
[26] X.W. Shan, H.D. Chen, Lattice Boltzmann model of simulating flows with multiple phases and components, Phys. Rev. E 47 (1993) 1815–1819.
[27] X.W. Shan, H.D. Chen, Simulation of nonideal gases liquid-gas phase transitions by the lattice Boltzmann equation, Phys. Rev. E 49 (1994) 2941–2948.
[28] M. Swift, W. Osborn, J. Yeomans, Lattice Boltzmann simulation of nonideal fluids, Phys. Rev. Lett. 75 (1995) 830–833.
[29] A.K. Gunstensen, D.H. Rothman, S. Zaleski, G. Zanetti, lattice Boltzmann model of immiscible fluids, Phys. Rev. A 43 (1991) 4320–4327.
[30] K.N. Premnath, J. Abraham, Three-dimensional multi-relaxation lattice Boltzmann models for multiphase flows, J. Comput. Phys. 224 (2007) 539–559.
[31] S.P. Dawson, S.Y. Chen, G.D. Doolen, lattice Boltzmann computations for reaction–diffusion equations, J. Chem. Phys. 98 (1993) 1514–1523.
[32] D.J. Holdych, J.G. Georgiadis, R.O. Buckius, Migration of a van der Waals bubble: Lattice Boltzmann formulation, Phys. Fluids 13 (2001) 817–825.
[33] M.R. Swift, E. Orlandini, W.R. Osborn, J.M. Yeomans, Lattice Boltzmann simulations of liquid–gas and binary fluid systems, Phys. Rev. E 54 (1996) 5041–5052.
[34] R.S. Maier, R.S. Bernard, D.W. Grunau, Boundary conditions for the lattice Boltzmann method, Phys. Fluids 8 (1996) 1788–1801.
[35] S. Succi, E. Foti, F.J. Higuera, Three-dimensional flows in complex geometries with the lattice Boltzmann method, Europhys. Lett. 10 (1989) 433–438.

[36] A.J.C. Ladd, Numerical simulations of particle suspensions via a discretized Boltzmann equation. Part 2. Numerical results, J. Fluids Mech 271 (1994) 311–339.
[37] O. Filippova, D. Hänel, Lattice-Boltzmann simulation of gas-particle flow in filters, Comput. Fluids 26 (1997) 697–712.
[38] C.H. Sun, Lattice-Boltzmann model for high speed flows, Phys. Rev. E 58 (1998) 7283–7287.
[39] M. De Cicco, S. Succi, G. Balla, Nonlinear stability of compressible thermal lattice BGK models, SIAM J. Sci. Comput. 21 (1999) 366–377.
[40] T. Kataoka, M. Tsutahara, Lattice Boltzmann method for the compressible Euler equations, Phys. Rev. E 69 (2004) 056702.1–056702.14.
[41] H.M. Wang, Numerical simulation of the ion-acoustic solitary waves in plasma based on lattice Boltzmann method, Adv. Space Res. 56 (2015) 1161–1168.
[42] H.M. Wang, A lattice Boltzmann model for the ion- and electron-acoustic solitary waves in beam-plasma system, Appl. Math. Comput. 279 (2016) 62–75.
[43] G.W. Yan, A lattice Boltzmann equation for waves, J. Comput. Phys. 161 (2000) 61–69.
[44] J.Y. Zhang, G.W. Yan, X.B. Shi, Lattice Boltzmann model for wave propagation, Phys. Rev. E 80 (2009) 026706.1–026706.13.
[45] M. Hirabayashi, Y. Chen, H. Ohashi, The lattice BGK model for the Poisson equation, JSME Int. J. Ser. B 44 (2001) 45–52.
[46] Z.H. Chai, B.C. Shi, A novel lattice Boltzmann model for the Poisson equation, Appl. Math. Model. 32 (2008) 2050–2058.
[47] H.M. Wang, G.W. Yan, B. Yan, Lattice Boltzmann model based on the rebuilding-divergency method for the Laplace equation and the Poisson equation, J. Sci. Comput. 46 (2011) 470–484.
[48] G.W. Yan, Studies of Burgers equation using a lattice Boltzmann method, Acta Mech. Sin. 31 (1999) 143–151.
[49] J.Y. Zhang, G.W. Yan, Lattice Boltzmann method for one and two-dimensional Burgers equation, Physica A 387 (2008) 4771–4786.
[50] G.W. Yan, L. Yuan, Lattice Bhatnagar–Gross–Krook model for the Lorenz attractor, Physica D 154 (2001) 43–50.
[51] J.G. Zhou, Lattice Boltzmann Methods for Shallow Water Flows, Springer-Verlag, Berlin Heidelberg, Germany, 2000.
[52] I. Ginzburg, Variably saturated flow described with the anisotropic lattice Boltzmann methods, Comput. Fluids 25 (2006) 831–848.
[53] S. Succi, Numerical solution of the Schrödinger equation using discrete kinetic theory, Phys. Rev. E 53 (1996) 1969–1975.
[54] S. Succi, Lattice quantum mechanics: an application to Bose- Einstein condensation, Int. J. Mod. Phys. C 9 (1998) 1577–1585.
[55] S. Palpacelli, S. Succi, Numerical validation of the quantum lattice Boltzmann scheme in two and three dimension, Phys. Rev. E 75 (2007) 066704.1–066704.13.
[56] S. Palpacelli, S. Succi, R. Spiggler, Ground-state computation of Bose–Einstein condensates by an imaginary- time quantum lattice Boltzmann scheme, Phys. Rev. E 76 (2007) 036712.
[57] L.H. Zhong, S.D. Feng, P. Dong, S.T. Gao, Lattice Boltzmann schemes for the nonlinear Schrödinger equation, Phys. Rev. E 74 (2006) 036704.1–036704.9.
[58] H.M. Wang, G.W. Yan, Lattice Boltzmann model for the interaction of $(2+1)$-dimensional solitons in generalized Gross–Pitaevskii equation, Appl. Math. Model. 40 (2016) 5139–5152.
[59] S. Chapman, T.G. Cowling, The Mathematical Theory of Non-uniform Gases, Cambridge University Press, Cambridge, 1970.